

Unraveling Vulnerabilities in Endocrine Therapy-Resistant HER2+/ER+ Breast Cancer

Authors:

Shaymaa Bahnassy¹, Hillary Stires², Lu Jin¹, Stanley Tam¹, Dua Mobin¹, Manasi Balachandran³,
Mircea Podar⁴, Matthew D. McCoy¹, Robert A. Beckman⁵, Rebecca B. Riggins^{1*}

Affiliations:

¹Department of Oncology, Lombardi Comprehensive Cancer Center, Georgetown University,
Washington, DC.

²Friends of Cancer Research, Washington, DC.

³University of Tennessee Medical Center, Knoxville, TN.

⁴Oak Ridge National Laboratory, Oak Ridge, TN.

⁵Departments of Oncology and of Biostatistics, Bioinformatics, and Biomathematics, Lombardi
Comprehensive Cancer Center and Innovation Center for Biomedical Informatics, Georgetown
University Medical Center, Washington, DC

***Corresponding Author:** Rebecca B. Riggins, 3970 Reservoir Rd NW, E412 Research Bldg,
Washington, DC 20057, email rbr7@georgetown.edu

18 **SUPPLEMENTAL MATERIALS and METHODS**

19 **Table S1:** List of primer sequences used for the detection of transcripts.

Gene	Primer Sequence	Reference
ESR1	Forward: 5'-AGAGGGGCATGGTGGAGATCTT-3' Reverse: 5'-CAAACCTCCTCTCCCTGCAGATT-3'	(1)
PGR	Forward: 5'-CAGTGGGCAGATGCTGTATT-3' Reverse: 5'-GGATCTGCCACATGGTAAGG-3'	
TIFF1	Forward: 5'-CCCTCCCAGTGTGCAAATAA-3' Reverse: 5'-GATCCCTGCAGAAGTGTCTAAA-3'	
ASPH	Forward: 5'-CATGGAGGACACAAGAATGGG-3' Reverse: 5'-CCAAACGACAGCTACAGATGT-3'	(2)
S100A4	Forward: 5'-AGTTCAAGCTCAACAAGTCAGAACTAA-3' Reverse: 5'-TCATCTGTCCTTTTCCCAAGA-3'	(3)
MARCKS	Forward: 5'-TCTCCTGTCCGTTGCTTTG-3' Reverse: 5'-CCAGTTCTCCAAGACCGCAG-3'	(4)
MDK	Forward: 5'-ATGCAGCACCGAGGCTTCCT-3' Reverse: 5'-ATCCAGGCTTGGCGTCTAGT-3'	(5)
ALOX15B	Forward: 5'-CAATGCCGAGTTCTCCTTCCATG-3' Reverse: 5'-TGATGTGCAGGGTGTATCGGGT-3'	(6)
SLC12A2	Forward: 5'-ATCAATTTTTTCAGTATTCCATGCATC-3' Reverse: 5'-ACGCCATCCTGGAGATTTTG-3'	(7)
DUSP6	Forward: 5'-AACAGGGTTCCAGCACAGCAG-3' Reverse: 5'-GGCCAGACACATTCCAGCAA-3'	(8)

TFAP2B	Forward: 5'-TGAAGATGCCAATAACAGCGGCA-3' Reverse: 5'-GGAGCAAAACACCTCGCCGGT-3'	(9)
IER3	Forward: 5'-AGTCTGGTGGTGGGTCGTAAGT-3' Reverse: 5'-GATGGAAGGATCTCACGGATCT-3'	(10)
TMEM205	Forward: 5'-GCAAATGTGGGTGACCTTCGTC-3' Reverse: 5'-GCAGAGGTTGATGAAGGCACAG-3'	
DHRS2	Forward: 5'-GGTGTCTACAATGTCAGCAAGA-3' Reverse: 5'-CACGCAGTTTACCCGGATGT-3'	
ACTB	Forward: 5'-AAGCCACCCCACTTCTCTCTAA-3' Reverse: 5'-CACCTCCCCTGTGTGGACTT-3'	(11)

20

21

SUPPLEMENTAL FIGURES and FIGURE LEGENDS

Figure S1. Effects of HER2- and ER-targeted therapies on ER expression and phosphorylation of HER2 in HER2+/ER+ LTEDs. (A-B) Western blot assessment of ER expression and phosphorylation of HER2 in BT474 LTEDs (A) and MM361 LTEDs (B) upon 6 h of treatment with either vehicle, 10 nM E2, 10 nM E2 + 100 nM ICI or 100 µg/ml T + 100 µg/ml P. Blots were analyzed by densitometry using ImageJ. Protein expressions were normalized to GAPDH and graphed as mean ± SEM from at least two independent experiments. One-way ANOVA followed by Dunnett's multiple comparison test was performed to compare groups and statistical significance is shown on the graph. The arrow on the MM361 LTEDB blot indicates correct molecular weight of ER (other bands are non-specific).

Figure S2. Breast tumors harboring mutated genes identified in MM361 LTED cells are associated with HER2+ status and lower PR expression. (A-B) Data were obtained from Razavi *et al.* (12) using cBioPortal for Cancer Genomics (<http://www.cbioportal.org/>, accessed on 11 May 2023). Stacked bar charts illustrate HER2 status (classified by FISH and IHC; thus HER2+ indicates *ERBB2*/HER2 amplification) (A) and PR status (B) distributions in breast tumors with and without mutational alterations in at least one gene in which we identified non-silent exonic mutation in LTED cells (mutated gene list in Table S2). Proportions were tested by chi-squared analysis. Number of samples and statistical significance are shown on the graph.

Figure S3. Cluster analysis of MM361 parental and LTED cell scRNAseq data. (A) UMAP plot of scRNAseq data grouped by unsupervised clustering (10 Principal Components, Resolution 0.5) into seven clusters (0-6) across parental and LTED cell lines. **(B-C)** Sankey plot (B) and tabular (C) representation of the number of sequenced cells belonging to each cluster. **Bold**

clusters **0** and **6** are enriched in LTED cells, while *italicized* clusters 2 and 5 are enriched in parental MM361 cells. **(D)** Top enriched biological processes in parental- (2, 5) and LTED-dominant (0, 6) cell clusters, respectively. Genes from clusters were analyzed by GSEA using the Hallmark and REACTOME gene sets, with FDR q-values <0.05. Specific clusters in which these gene sets were enriched are indicated.

Figure S4. scRNAseq expression of *ESR1* and *ERBB2* in MM361 parental and LTED cells. UMAP plot of scRNAseq data shaded by expression of the indicated genes.

Figure S5. Ferroptosis-related genes in MM361 LTEDs. Analysis of the ferroptosis database (FerrDb V2) (13) and other literature search show that 13 of our DEGs are ferroptosis-related. Red and blue indicate upregulated and downregulated genes, respectively.

Figure S6. Dual targeting of HER2 and GPX4 increase cell death of BT474 LTEDs. (A) Representative immunoblot of three independent experiments showing enhanced expression of GPX4 protein in BT474 LTEDs. **(B-C)** Sytox staining experiments show that TP + RSL3 induces the highest cell death in BT474 LTEDs. Cells treated with either vehicle, 1 µg/ml TP, 250 nM RSL3 or a combination of both for 72 h then stained with Hoechst to monitor total cell number (gray nuclei), and Sytox green to monitor dead cells (green nuclei). (B) Cell death representative images and (C) quantifications from two independent experiments with at least 10 fields being analyzed for each. Data presented as mean ± SEM of cell death percentages using one-way ANOVA followed by Tukey's multiple comparison test. * $p < 0.05$ and *** $p < 0.001$ were considered statistically significant.

Figure S7. Effects of TP and RSL3 on protein expression of ferroptosis lipid peroxidation markers (4-HNE and MDA). MM361 LTED cells were treated with either vehicle, 1 µg/ml T + 1 µg/ml P, 1 µM RSL3 or a combination of both for 72 h then whole cell lysates were analyzed by western blot analysis. Immunoblots are a representation of two independent experiments. Blots were analyzed by densitometry using ImageJ and protein expression was normalized to vinculin.

REFERENCES

1. De Amicis F, Russo A, Avena P, Santoro M, Vivacqua A, Bonofiglio D, Mauro L, Aquila S, Tramontano D, Fuqua SAW, Andò S. In vitro mechanism for downregulation of ER- α expression by epigallocatechin gallate in ER+/PR+ human breast cancer cells. *Mol Nutr Food Res*. 2013;57(5):840-853.
2. Qu Y, Qi L, Hao L, Zhu J. Upregulation of circ-ASPH contributes to glioma cell proliferation and aggressiveness by targeting the miR-599/AR/SOCS2-AS1 signaling pathway. *Oncol Lett*. 2021;21(5):388.
3. Liu Y, Men C, Xu Y, Zhao K, Luo L, Dong D, Yu Q. Clusterin promotes growth and invasion of clear cell renal carcinoma cell by upregulation of S100A4 expression. *Cancer Biomarkers*. 2018;21:915-923.
4. Kim YE, Kim EK, Song MJ, Kim TY, Jang HH, Kang D. SILAC-Based Quantitative Proteomic Analysis of Oxaliplatin-Resistant Pancreatic Cancer Cells. *Cancers (Basel)*. 2021;13(4).
5. Erdogan S, Turkekul K, Dibirdik I, Doganlar O, Doganlar ZB, Bilir A, Oktem G. Midkine downregulation increases the efficacy of quercetin on prostate cancer stem cell survival and migration through PI3K/AKT and MAPK/ERK pathway. *Biomed Pharmacother*. 2018;107:793-805.
6. Li C, Zhang Y, Liu J, Kang R, Klionsky DJ, Tang D. Mitochondrial DNA stress triggers autophagy-dependent ferroptotic death. *Autophagy*. 2021;17(4):948-960.
7. Wright PK, May FE, Darby S, Saif R, Lennard TW, Westley BR. Estrogen regulates vesicle trafficking gene expression in EFF-3, EFM-19 and MCF-7 breast cancer cells. *Int J Clin Exp Pathol*. 2009;2(5):463-475.
8. Song H, Wu C, Wei C, Li D, Hua K, Song J, Xu H, Chen L, Fang L. Silencing of DUSP6 gene by RNAi-mediation inhibits proliferation and growth in MDA-MB-231 breast cancer cells: an in vitro study. *Int J Clin Exp Med*. 2015;8(7):10481-10490.
9. Wang L, Wang C, Wu T, Sun F. Long non-coding RNA TP73-AS1 promotes TFAP2B-mediated proliferation, metastasis and invasion in retinoblastoma via decoying of miRNA-874-3p. *J Cell Commun Signal*. 2020;14(2):193-205.
10. Labhart P, Karmakar S, Salicru EM, Egan BS, Alexiadis V, O'Malley BW, Smith CL. Identification of target genes in breast cancer cells directly regulated by the SRC-3/AIB1 coactivator. *Proc Natl Acad Sci U S A*. 2005;102(5):1339-1344.
11. Santolla MF, Talia M, Maggiolini M. S100A4 Is Involved in Stimulatory Effects Elicited by the FGF2/FGFR1 Signaling Pathway in Triple-Negative Breast Cancer (TNBC) Cells. *International Journal of Molecular Sciences*. 2021;22(9):4720.
12. Razavi P, Chang MT, Xu G, Bandlamudi C, Ross DS, Vasan N, Cai Y, Bielski CM, Donoghue MTA, Jonsson P, Penson A, Shen R, Pareja F, Kundra R, Middha S, Cheng ML, Zehir A, Kandoth C, Patel R, Huberman K, Smyth LM, Jhaveri K, Modi S, Traina TA, Dang C, Zhang W, Weigelt B, Li BT, Ladanyi M, Hyman DM, Schultz N, Robson ME, Hudis C, Brogi E, Viale A, Norton L, Dickler MN, Berger MF, Iacobuzio-Donahue CA, Chandarlapaty S, Scaltriti M, Reis-Filho JS, Solit DB, Taylor BS, Baselga J. The Genomic Landscape of Endocrine-Resistant Advanced Breast Cancers. *Cancer Cell*. 2018;34(3):427-438 e426.
13. Zhou N, Yuan X, Du Q, Zhang Z, Shi X, Bao J, Ning Y, Peng L. FerrDb V2: update of the manually curated database of ferroptosis regulators and ferroptosis-disease associations. *Nucleic Acids Res*. 2023;51(D1):D571-D582.

Fig S1.

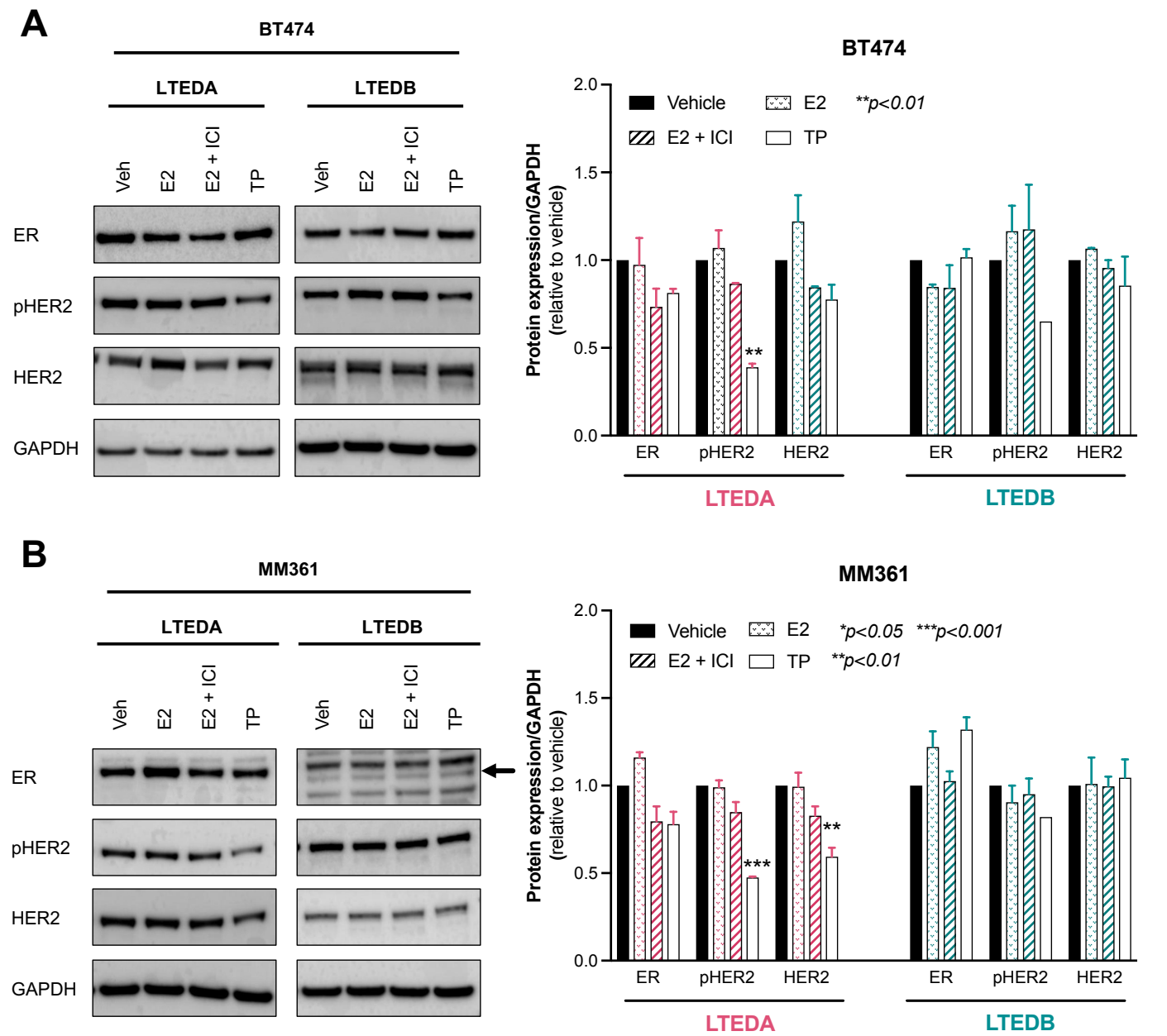
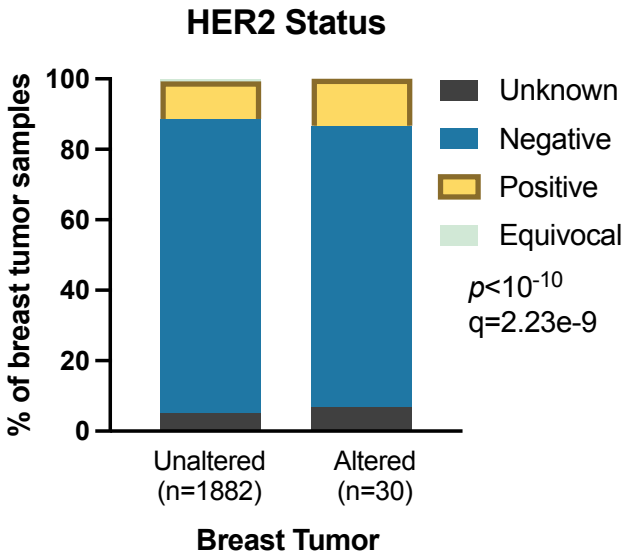


Figure S2.

A



B

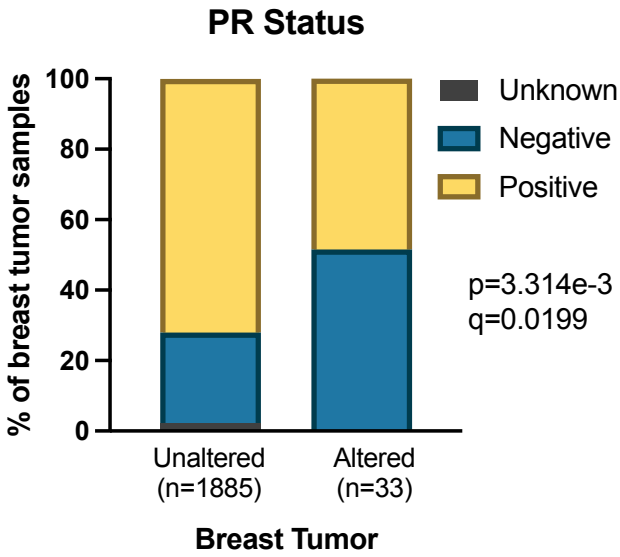


Figure S3.

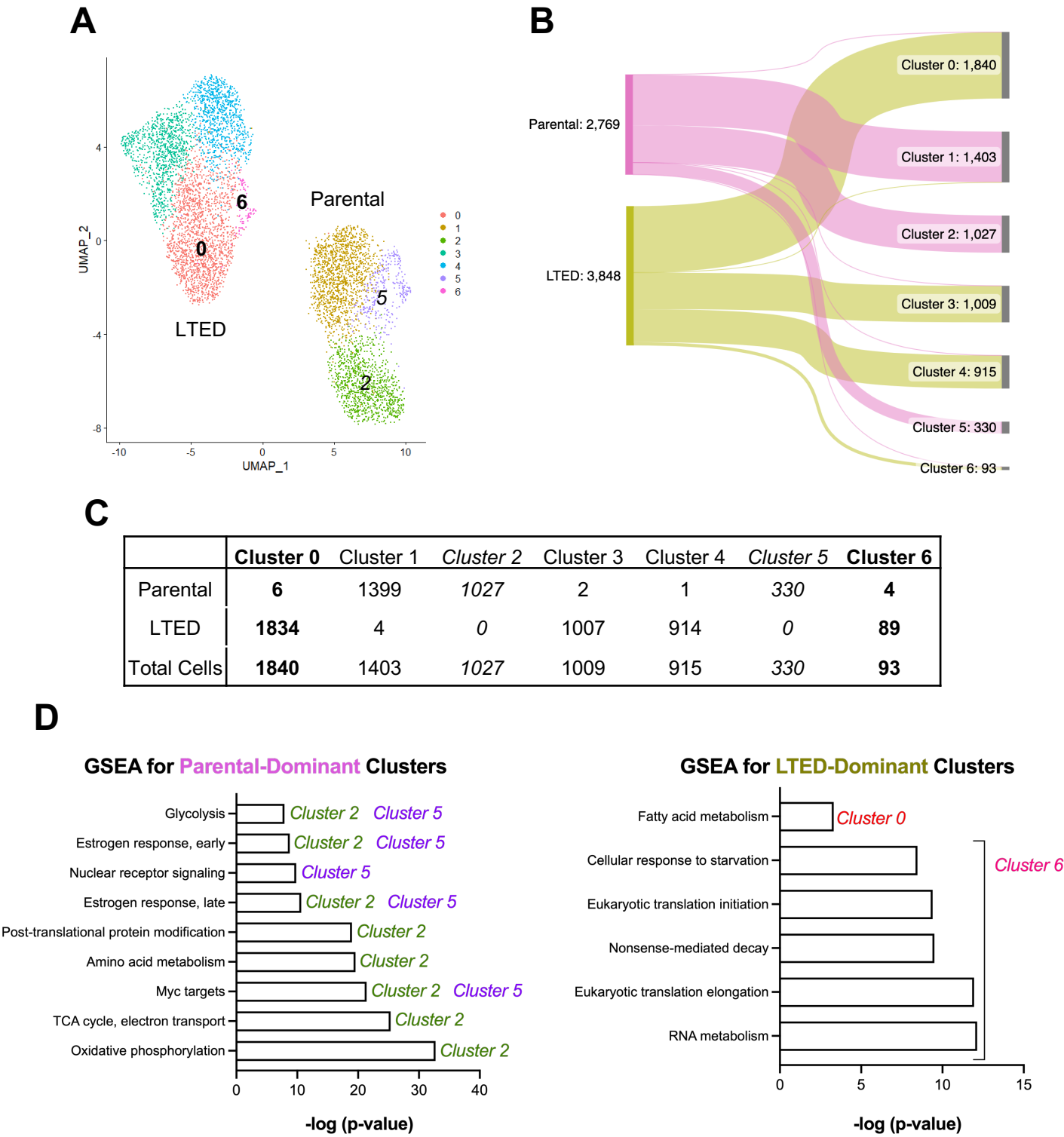


Figure S4.

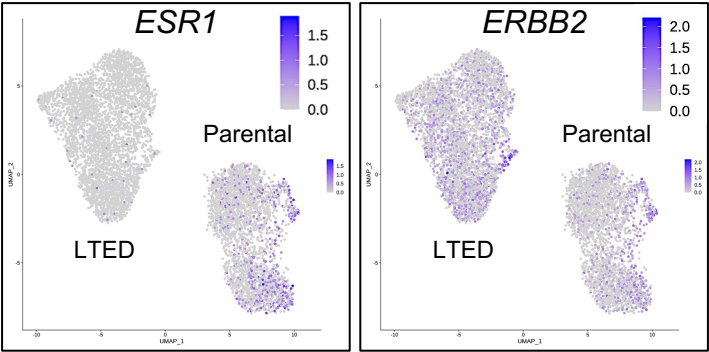


Figure S5.

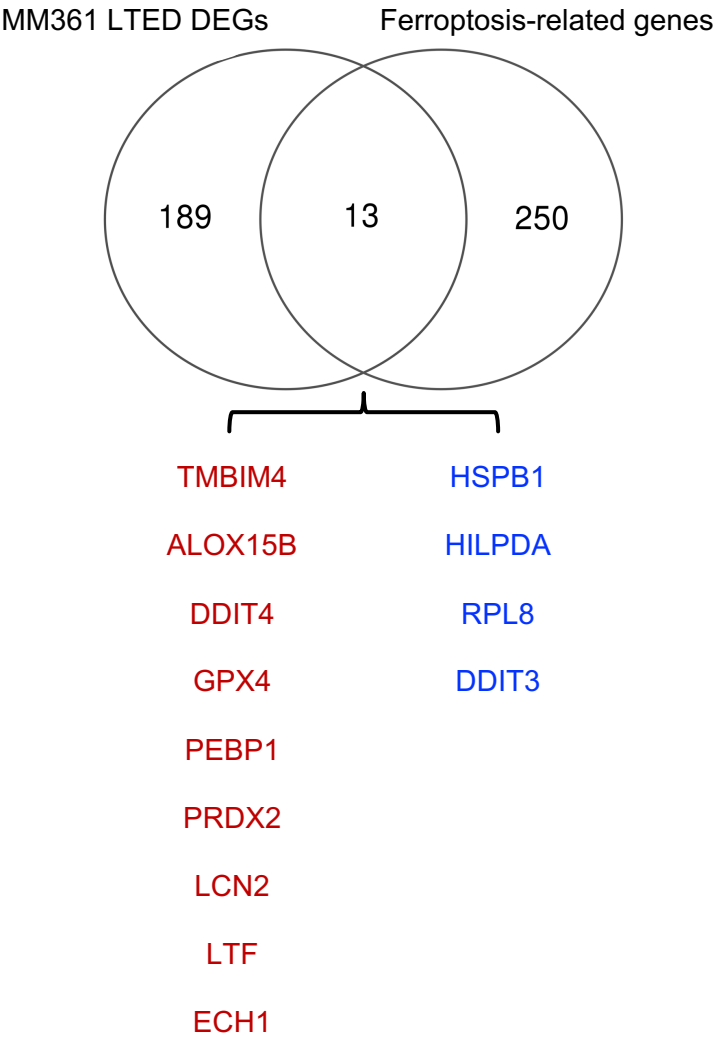


Fig S6.

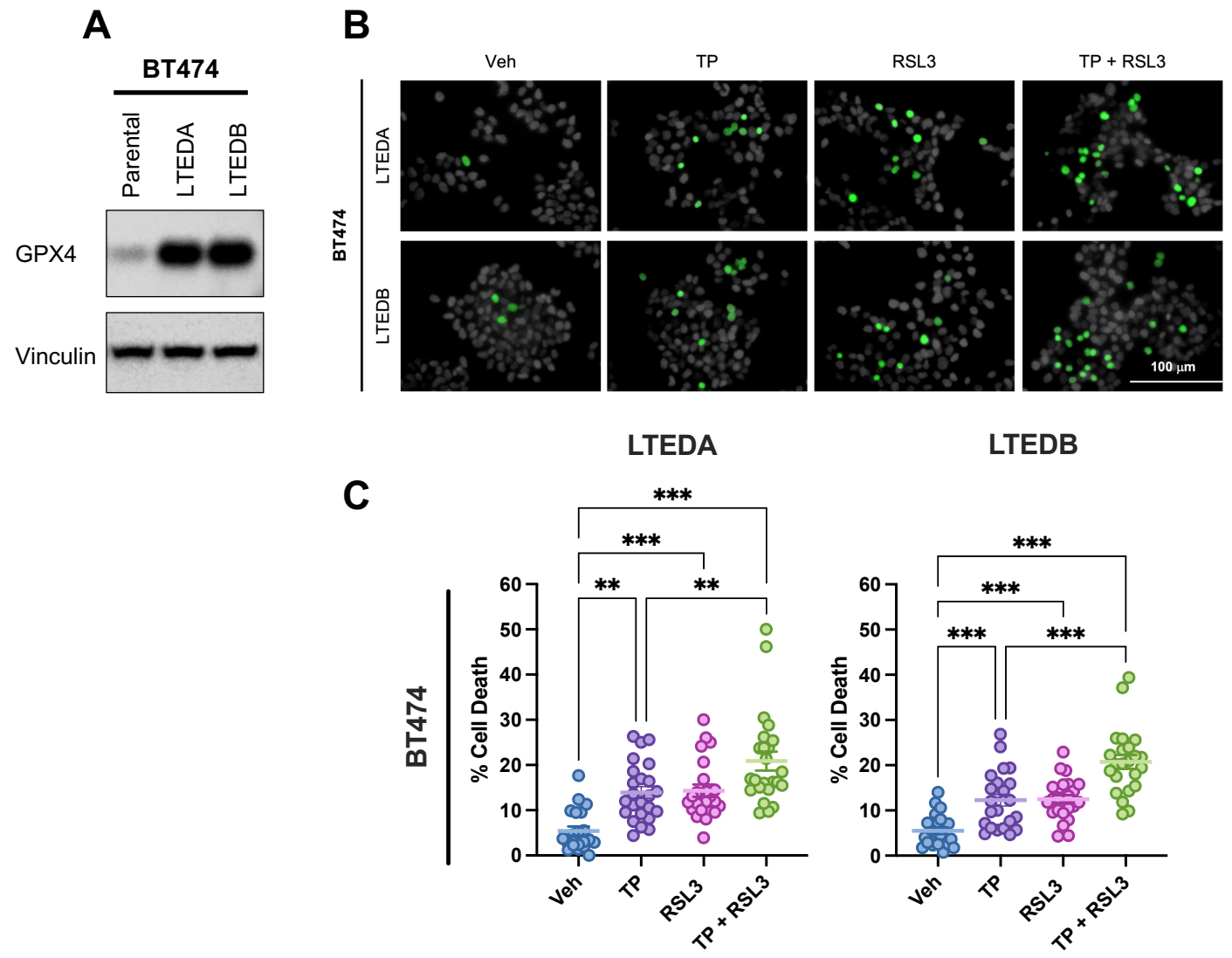


Figure S7.

